CHAPTER 3

Microscopic Methods for Measuring the Elasticity of Gel Substrates for Cell Culture: Microspheres, Microindenters, and Atomic Force Microscopy

Margo T. Frey,* Adam Engler,† Dennis E. Discher,† Juliet Lee,‡ and Yu-Li Wang*

*Department of Physiology
University of Massachusetts Medical School
Worcester, Massachusetts 01605

†Department of Chemical and Biomolecular Engineering
University of Pennsylvania
Philadelphia, Pennsylvania 19104

‡Department of Molecular and Cell Biology
University of Connecticut
Storrs, Connecticut 06269

METHODS IN CELL BIOLOGY, VOL. 83

0091-679X/07 $35.00
DOI: 10.1016/S0091-679X(07)83003-2

Abstract

In conjunction with surface chemistry, the mechanical properties of cell culture substrates provide important biological cues that affect cell behavior including growth, differentiation, spreading, and migration. The phenomenon has led to the increased use of biological and synthetic polymer-based flexible substrates in cell culture studies. However, widely used methods for measuring the Young's modulus have proven difficult in the characterization of these materials, as they tend to be relatively thin, soft, hydrated, and tethered to glass substrates. Here we describe three methods that have been applied successfully to probe the flexibility of soft culture substrates.

I. Introduction

A number of chapters in this volume have highlighted the important influence of soft substrates on cell adhesion, cell structure, and cell mechanics. These studies rely on reliable measurements of the Young's modulus (Chapter 1 by Janmey *et al.*, and Chapter 2 by Kandow *et al.*, this volume) of the culture substrate. However, classical methods for measuring material elasticity and other mechanical properties generally require macroscopic samples, often of a specific geometry, while gels intended for cell culture are generally formed as a thin layer adhered to the culture dish. Reliable measurements of such gels must be performed *in situ* because (1) gels can be so soft that macroscopic samples are difficult to handle; (2) gels are hydrated and sometimes temperature sensitive so smaller samples are more homogeneous and easier to control; (3) gels are often tethered to the underlying cover glass, which may affect the expansion or compression of gels; and (4) with cells adhering to the gel surfaces, measuring the elasticity of the gel surface instead of the bulk will provide values more relevant to cell behavior.

The purpose of this chapter is to describe three microscopic methods suitable for measuring the elasticity of gel substrates *in situ*. While all of them are based on Hertz contact mechanics (Hertz, 1882), namely the indentation in response to forces exerted with a probe of known geometry, they differ substantially in cost, simplicity, and resolution. Since indentations with metal microspheres under gravity and with atomic force microscopy (AFM; Chapter 15 by Radmacher, this volume) have been described in the literature, the description here will be limited to several key aspects critical to gel measurements. The method of microneedle indentation, which combines features of the two other methods, was developed recently as both a qualitative and a quantitative tool for probing substrates with modulatable mechanical properties. Since it has never been described, sufficient details will be provided for reproduction.

With all three methods, the measurements should be performed on fully acclimated substrates since hydrogel substrates are often sensitive to buffer conditions and temperature. In addition, the thickness of the testing sample should be close to that used for actual experiments. This is particularly important for polyacrylamide

gels, since the surface rigidity decreases progressively with increasing thickness due to the covalent bonding of the gel to the coverslip to limit gel swelling and prevent detachment (Chapter 2 by Kandow *et al.*, this volume).

II. Probing with Microspheres Under Gravitational Forces

The microsphere indentation method is performed by measuring the indentation depth of a relatively heavy metal microsphere placed on top of the substrate (Lo *et al.*, 2000). It works with a high degree of reproducibility for both polyacrylamide and gelatin substrates with Young's moduli of $E \sim 2.2$–33 kPa. Hydrogel substrates are prepared with embedded fluorescent latex beads 0.1–0.2 μm in diameter. As the method relies strongly on the ability to focus accurately on the substrate surface, using these beads as markers, the beads may be confined to the top surface using the approach described in Chapter 2 by Kandow *et al.*, this volume. Since hydrogel substrates are often sensitive to buffer conditions and temperature, all the measurements should be performed with fully acclimated substrates (this also applies to the two other methods). With the substrate seated on the stage of an inverted microscope, a stainless steel microsphere of known diameter (0.3–0.62 mm) and density (e.g., 7.72 g/cm^3 for Pen grade 420SS stainless steel, Hoover Precision, East Granby, Connecticut) (Fig. 1) is gently placed near the field of observation with a pair of fine forceps. The measurement is made using an objective with a working distance larger than the thickness of the gel and with a numerical aperature as high as possible. Indentation is determined using the calibrated fine focus control of the microscope. For most microscopes the fine focus knob is marked in 1-μm increments, which can be confirmed and/or recalibrated by focusing through a second glass coverslip of known thickness with permanent ink marks on either side.

To avoid problems with backlash of the gears, the microscope should be focused first beneath and near the center of the metal microphere to mark the height of the indented surface, which is recognized as the region with maximal indentation. After the microscope is focused on the fluorescent beads near the gel surface of

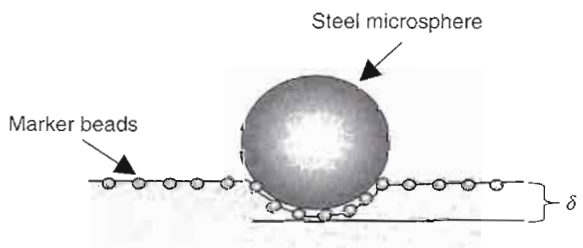

Fig. 1 Illustration of the indentation, δ, made by a steel microsphere placed on a gelatin substrate embedded with marker beads.

this region, the microsphere is removed with a magnet and the ensuing vertical movement of the gel surface measured by refocusing on the same group of fluorescent beads. Measurements are taken at five random locations on the substrate, and the average indentation is used to calculate the Young's modulus (E) given by the Hertz equation [Eq. (1)] (Hertz, 1882):

$$E = \frac{3(1 - \nu^2)f}{4r^{1/2}\delta^{3/2}} \tag{1}$$

where r is the bead radius, f is the force applied by the steel ball, δ is the indentation of the substratum, and ν is the Poisson ratio of the hydrogel, assumed here to be 0.5 for gelatin (Li *et al.*, 1993) and 0.45 for polyacrylamide (Section IV.F). Note that f equals the gravitational forces minus the buoyancy, which equals the weight of the liquid displaced by the volume of the microsphere. By this method, the Young's modulus for 3% gelatin gels should be ~3 kPa.

Although the microsphere indentation method is simple and cost-effective, it tends to yield Young's moduli higher than those obtained with the other two methods. One possible source of error is that if δ is a significant fraction of the thickness of the gel, then the rigid glass surface below the gelatin or other gel substrate will significantly limit δ. Overestimation of E can also occur due to high systematic error at low indentation depths, for example, from a higher actual contact area than that expected from the Hertz equation (Yoffe, 1984; discussed later). To minimize these problems, the density and radius of microspheres should be chosen such that $\delta < 0.2t$ and $>0.3r$, where t is the thickness of the gel. In practice, the versatility of the microsphere indentation method is limited by the availability of microsphere to meet these criteria, particularly for stiff gels.

III. Atomic Force Microscopy

Several key aspects of the microsphere indentation technique are implemented and extended in a commercially available, high-resolution instrument known as the AFM. A number of designs are available from different AFM manufacturers, with prices starting at about half the cost of an inverted optical microscope. While imaging applications of AFM are relatively well known (Bennig *et al.*, 1986), the AFM in the "force mode" is highly suited to detailed mechanical assessments at microscale resolution (Weisenhorn *et al.*, 1989).

The key component of the AFM is a microfabricated flexible cantilever with a micrometer scale probe tip that is generally pyramidal in shape but can also be a sphere. These cantilevers are purchased individually or as wafers, with a spring constant that comes precalibrated to within about 50%; a more precise calibration is done on each cantilever at the time of use by standard methods supplied by the instrument manufacturer. The cantilever is displaced by a piezoelectric device to press the tip into an immobilized sample material, and the forced deflection of the

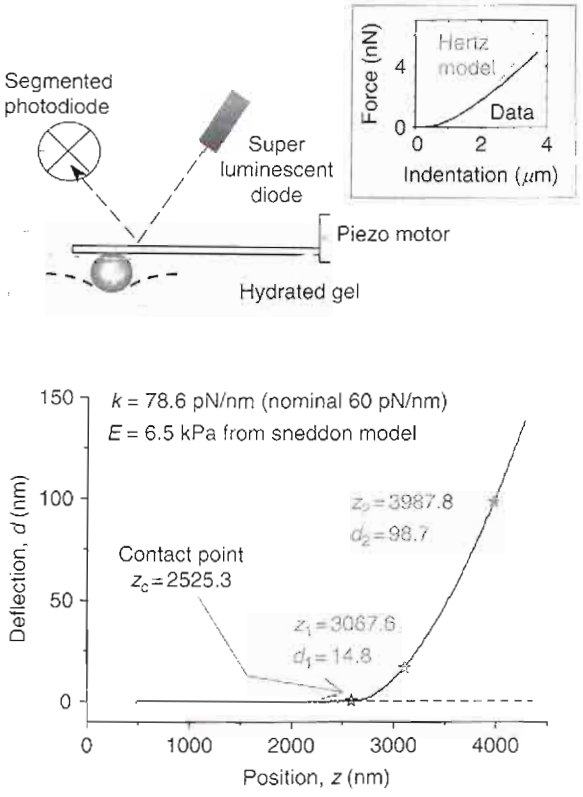

Fig. 2 Application of atomic force microscopy for probing the mechanical properties of gel substrates, by pressing into the surface and analyzing the resulting deflection. Light from a superintensified diode (or laser) is reflected off the end of the cantilever onto a segmented photodiode detector that magnifies small tip deflections into a detectable signal. When pressing the tip into the sample, indentation can be determined as the difference between tip deflection and the cantilever position and then plotted versus the force required to create the tip's deflection. The force–indentation plot can then be fit with a Hertz-type model (inset plot). The lower plot illustrates how the point of contact is determined from Eq. (4) in the text.

cantilever is measured by reflection of a laser off the backside of the cantilever and onto a position-sensitive photodetector (Fig. 2). Indentation of the material, δ, is determined by subtracting the deflection, d, of the cantilever from the distance driven by the piezoelectric device, z. The deflection is converted to force using the cantilever calibration curve, and force–indentation data can then be plotted as shown in the upper inset of Fig. 2.

A first consideration for an AFM cantilever is its spring constant, k. Spring constants have units of force per distance and range from relatively rigid (k = 100–1000 pN/nm) to soft (5–100 pN/nm). The latter yields a better signal-to-noise ratio when performing measurements on soft gel samples. Also of importance is the tip geometry, for example, pyramidal with different sharpness or spherical with

different radii. Each probe type imparts a specific deformation field when indenting a material and as such, each has a mechanical model associated with it. For cantilevers with spherical tips such as those with $r = 2.5$-μm borosilicate beads mounted on 60-pN/nm cantilevers available commercially (e.g., Bioforce Nanoscience, Ames, Iowa), Eq. (1) given above for indentation is used, although the fit of f versus δ from AFM is conducted over many data points collected over just a few micrometers of indentation.

Pyramidal tips (of shape V) have different degrees of tip sharpness, and blunted tips are usually preferred for force mode (not so for imaging) as blunted tips tend to distribute the deformation field over a larger contact surface, minimizing the strain and potential damage to the sample. The relationship between the indentation force, f, and the deformation, δ, may be approximated with an axisymmetric cone model (Sneddon, 1965).

$$f = \left[\frac{2 \tan(\alpha)}{\pi}\right]\left[\frac{E}{1 - \nu^2}\right]\delta^2 \tag{2}$$

where α is the opening angle of the pyramid tip (i.e., how tapered the tip is; other symbols are the same as defined before). Blunted tips typically have an opening angle, α, of 35°, whereas sharpened tips have an angle of 18°. Note that the smaller contact area with the pyramidal tip relative to a spherical tip means that the indentation force scales more strongly with deformation, δ (as δ^2 rather than $\delta^{3/2}$). The difference gives spherical probes an advantage, as it translates to lower strains that allow proper corrections for soft, thin films below 20 μm (Dimitriadis *et al.*, 2002; Engler *et al.*, 2004a).

To measure E of hydrogels, samples are indented at a relatively modest rate of cantilever displacement 0.2–2.0 μm/sec ($= dz/dt$), which is generally sufficient to explore elastic rather than viscoelastic properties of substrates (Mahaffy *et al.*, 2000). The first step in determining the Young's modulus is to pinpoint when the tip first makes contact with the substrate, referred to as the contact point. While this is easy for a hard material, the transition for soft materials can be less obvious, but a formula from Domke and Radmacher (1998) can be used for such determination. It utilizes the deflection (d)–position (z) plot, by fitting the curve near two extremes of the region where the curve is to be used for rigidity analysis, and calculating the point of interception with the x-axis [Eq. (3)].

$$\text{Contact point} = \left(\frac{(d_2/d_1)^a[(z_2 - d_2) - (z_1 - d_1)]}{1 - (d_2/d_1)^a}\right) \tag{3}$$

The exponent $a = 1/2$ for a cone (approximating a pyramidal tip) and $a = 2/3$ for a sphere. With a properly chosen range of analysis—which is most accurate for a cantilever deflection range $d \sim 10$–100 nm as shown between the two gray stars in the lower plot of Fig. 2—the contact point calculated from Eq. (3) should accurately reflect where indentation starts. The difference between tip positions, starting from the contact point and moving down into the sample, generates the tip's actual deflection by the material, which is then converted into force with the force–deflection

calibration curve and plotted against the indentation of the material. This force–indentation relationship may then be fit with the Hertz model for spherical tips or the Sneddon model for sharpened tips (Hertz, 1882; Sneddon, 1965), generally up to 2 μm of tip indentation, to determine E (Domke and Radmacher, 1998; Engler *et al.*, 2004a; Rotsch *et al.*, 1999).

A number of qualifications and conditions apply to such analyses. For example, for thin gels probed with spherical tips, a developed thin film approximation worked well (Dimitriadis *et al.*, 2002). Also, during measurement, attention should be paid to instrument parameters including indentation velocity, indentation distance, and data sampling rate. An example of such a relationship and fit is displayed as an inset in Fig. 2. For thick films, the resulting values of E typically do not depend on the range of indentation depth, but for thin films the measurements typically only fit the Hertz model at small indentations (Domke and Radmacher, 1998). Therefore, the range of analysis should be chosen according to the application.

The main drawback of AFM is the setup cost, and the limited longevity of the probe due to contaminations, which require replacement and calibration of new probes. Measurements of soft hydrogels can also be affected by adhesive interactions between the tip and the gel (Zhao *et al.*, 2003), which can bias the estimate of contact point. Additionally, unless the AFM is built on top of a high-quality light microscope, it will be necessary to move the sample between two different instruments to conduct both microscopic cellular studies and stiffness measurements of the gel. A third instrument may also be necessary to confirm gel thickness, required for a thin film correction of gels <20 μm in thickness (Richert *et al.*, 2004).

IV. Probing with Spherically Tipped Glass Microindenters

To address some of the limitations of microsphere indentation and AFM, a new approach was recently developed that uses a flexible glass microneedle with a spherical tip to probe the gel. The method is identical to AFM in principle, measuring the indentation of the gel in response to calibrated forces exerted at a spherical tip. However, the position of the probe and the indentation of the material are measured through an optical microscope with a calibrated focusing mechanism in conjunction with a micromanipulator. This allows both qualitative and quantitative measurements to be performed "*in situ*" on the microscope stage. The method may be viewed as an extension of an approach described by Lee *et al.* (1994), modified to incorporate Hertz contact physics for more reliable measurements. In addition, the method is closely related to the nanonewton force apparatus described in Chapter 18 of Davidson and Keller, this volume, and to the microindenter method described by Jacot *et al.* (2006).

The measurement is performed on a light microscope with a coupled imaging device. It is essential that the focusing mechanism move the objective lens, rather than the stage. The optimal objective lens should have a sufficient working distance to

image the surface of the hydrogel, and as high a numerical aperture as possible to give a shallow depth of field. Optimally the microscope should be equipped with a motorized focusing mechanism and fluorescence optics. In addition, the method requires a micropipette puller, a microforge, and a micromanipulator with a fine, precise vertical control. Although specific instrument models are given in the description below, a range of designs by different manufacturers, in addition to simpler custom-built devices, may be acceptable. The results may be analyzed manually, or using programs written in Excel or MatLab (available on request).

A. Preparation and Calibration of the Spherically Tipped Microindenter

A borosilicate glass capillary tube, 1.2 mm OD × 0.9 mm ID (Frederick Haer & Co., Bowdoinham, Maine), is first pulled into a thin fiber with a micropipette puller (Vertical Pipette Puller, Model 720, David Kopf Instruments, Tujunga, California). The heating and pulling settings on the puller are adjusted to create a long taper, about 15–20 mm from the beginning of the taper to the tip. A microforge (MF-900, Narishige Co., Ltd., Tokyo, Japan) is then used to melt the tip into a semispherical shape ~60–80 μm in diameter (Fig. 3A). Heat is also applied to the region ~150 μm from the tip to create a bend of ~45° (Fig. 3B). The spring constant of the microindenter may be varied over a wide range by experimenting with different glass materials, capillary sizes, and taper lengths.

B. Calibration of the Microscope and Micromanipulator

The magnification factor of the optical system should be calibrated with a micrometer standard to obtain the dimension imaged by each pixel, in micrometer per detector pixel. Vertical movement of the microscope focusing mechanism and the micromanipulator must be calibrated with a precision better than 0.5 μm. Calibration of the microscope-focusing knob may be performed by directly measuring a sample of known thickness, as described in the section of microbead

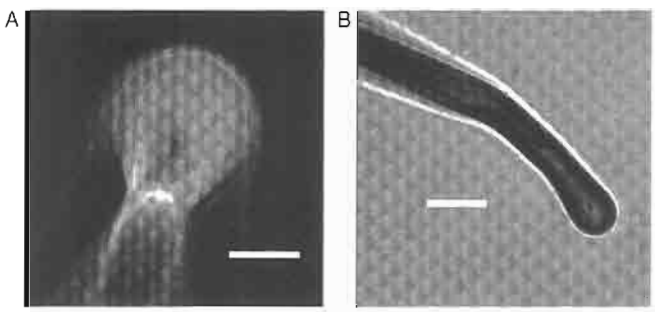

Fig. 3 Microindenter with a spherical tip, as viewed from the top (A, scale bar is 25 μm) or side (B, scale bar is 100 μm).

indentation. Once the focusing knob is calibrated, the movement of micromanipulator (a Leitz mechanical micromanipulator in this case) may be calibrated accordingly. This is performed by first focusing on a needle mounted on the micromanipulator (a Leitz mechanical micromanipulator in this case). The needle is then moved up by a known number of increments (e.g., 10 divisions on the micromanipulator knob or 45° turn), and the image of the needle is brought back into focus, keeping track of the position on the microscope focusing mechanism. These positions on the microscope are converted into distance according to the calibration of the focusing mechanism, and into the distance per micromanipulator increment.

C. Characterization and Calibration of the Microindenter

The first step in microindenter calibration is to obtain the radius r of the spherical tip, by taking an image and converting the radius in pixels into micrometers using the magnification factor obtained above. The next step is to collect a reference image of the microindenter, which is the phase-contrast image of the probe as the microscope is focused precisely on the bottom surface of the spherical tip.

The reference image is collected by pushing the microindenter against a glass surface sprinkled with 1-μm diameter fluorescent beads (FluoSpheres, Molecular Probes, Eugene, Oregon). The spherically tipped microindenter is mounted on the micromanipulator, at the tilting angle to be used for probing the gel and with the tip pointing down (see below), and is lowered slowly until the spherical tip just starts to thrust forward. This is the position where its bottom surface makes initial contact with the glass surface. Under the same magnification and optical conditions as will be used for probing the hydrogel (e.g., with an objective lens of 40×, 0.75 NA), bring the beads on the glass surface to sharp focus in fluorescence optics. Note that the use of fluorescence optics allows more precise focusing, although the beads can be readily visualized in phase-contrast optics. A phase-contrast image of the probe is then recorded. This image must be replaced again each time the microindenter is removed and remounted on the micromanipulator.

The spring constant of the microindenter is determined by measuring the bending after hanging a number of known weights near the tip. Basically, the microindenter is rotated such that the tip is pointing up, in order to hang a series of weights near the tip. The deflection (d) of the microindenter is measured using the focusing mechanism of the microscope (Fig. 4) and the spring constant, k, is determined from Hooke's law, $f = kd$ (Fig. 4C), where f is the gravitational force of the weight. The detailed procotol is given below.

1. Prepare a series of weights from thin electric wires of several different sizes, for example, by untwisting and separating individual conductors from thin telephone wires. Cut a piece 5–10 cm in length, measure the exact weight, and calculate the weight per mm. To match the stiffness of the microindenter, the linear density of the wire should generally be <0.1 mg/mm. Cut short pieces ~5 mm in length,

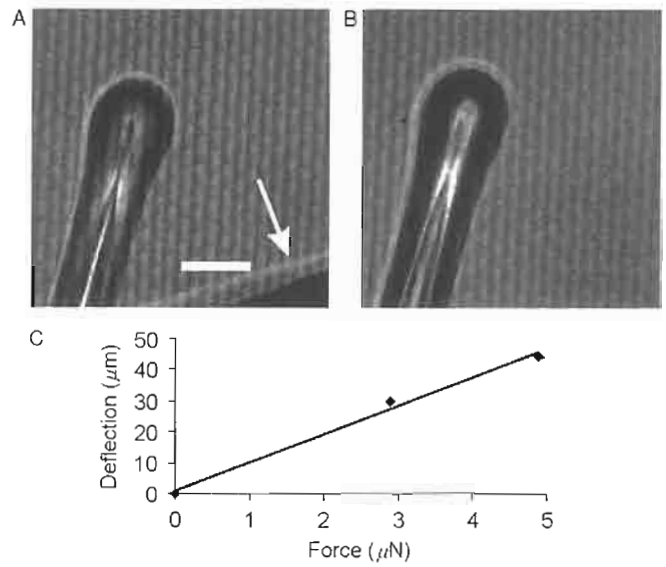

Fig. 4 Determination of the spring constant of the microindenter. The probe is deflected under applied weight load (A, arrow), and becomes out of focus on removal of the weight (B). Scale bar is 50 μm. The amount of deflection is determined from the change in focal plane and is plotted against the applied force (C).

and calculate the exact weight forces (f in nN = 9.81 × length in mm × density in mg/mm × 1000). Bend the wire into a V shape and bend one of the legs forward to facilitate handling.

2. Mount the microindenter on the micromanipulator at exactly the angle to be used for measuring the gel. As the sample typically sits on the bottom of a chamber, the angle of the microindenter will be limited by the accessibility to the sample. Therefore, even though this calibration does not require a sample chamber, it would be helpful to place one underneath the microindenter, both to monitor the approaching angle and to catch the calibrating weight that is blown off the microindenter during the calibration.

3. Rotate the microindenter and make sure that its bent tip is pointing *up*, which should be obvious by focusing the microscope up and down. In addition, no kink should be visible from its lateral profile under the microscope (compare Figs. 4A vs 3B).

4. Center and focus at the tip of the microindenter using low magnification, for example 10×.

5. Hang a wire weight on the microindenter with a pair of fine forceps, somewhere not too far from the tip. Gently tap the micromanipulator until the weight slips near the tip and gets caught at the bend. Make sure it does not touch the sample chamber. Monitor the last part of tapping under the microscope.

6. Switch to the magnification to be used for measuring the gel, or as high as the working distance of the lens allows (the tip of the microindenter is several millimeters above the objective lens, due to the upward bend and to the dangling calibration weight). Bring the tip to focus and record an image (Fig. 4A).

7. Tap or blow the weight off the tip of the needle. The tip of the microindenter becomes out of focus (Fig. 4B).

8. Adjust the microscope focus to restore the sharp image of the tip of the microindenter (image to match Fig. 4A). This step is best performed by collecting a stack of optical sections with a motorized focusing mechanism, and searching for the image in the stack that best matches the weighted image. Using the calibrated focusing knob, determine the distance of vertical movement, d.

9. Repeat the measurement with different weights.

10. Plot d as a function of f. Stiffness, k, is determined from the slope of the f–d curve (Fig. 4C).

D. Measurement of the Indentations of Hydrogels in Response to Forces of the Microindenter

Qualitative monitoring of the change in material properties may be carried out simply by imaging the tip of a stationary microindenter, which becomes out of focus when the flexibility changes. This is an excellent tool for developing modulatable materials, as one can easily visualize the change in stiffness.

For quantitative measurement, E of the gel is calculated from its indentation as a function of forces exerted by the microindentor using the Hertz equation. To minimize error (discussed later) and to yield results relevant to actual experimental conditions, the sample thickness should be in the range of 100–150 μm. The following procedure is designed to facilitate consistent measurement of the position of the microindenter, the point of contact with the gel, and the resulting gel indentation. See Fig. 5 for the explanation of various symbols and the relationship between the probe and the sample.

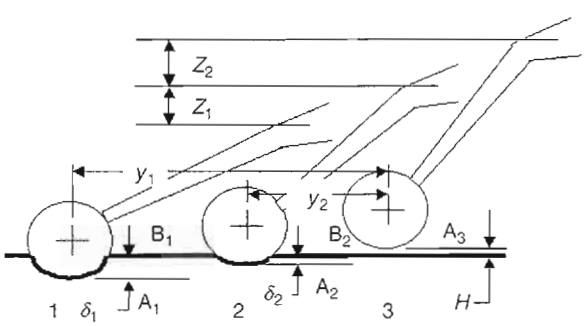

Fig. 5 Schematic of gel flexibility measurement using spherically tipped microindentation. See text for the definition of various positions marked by letters.

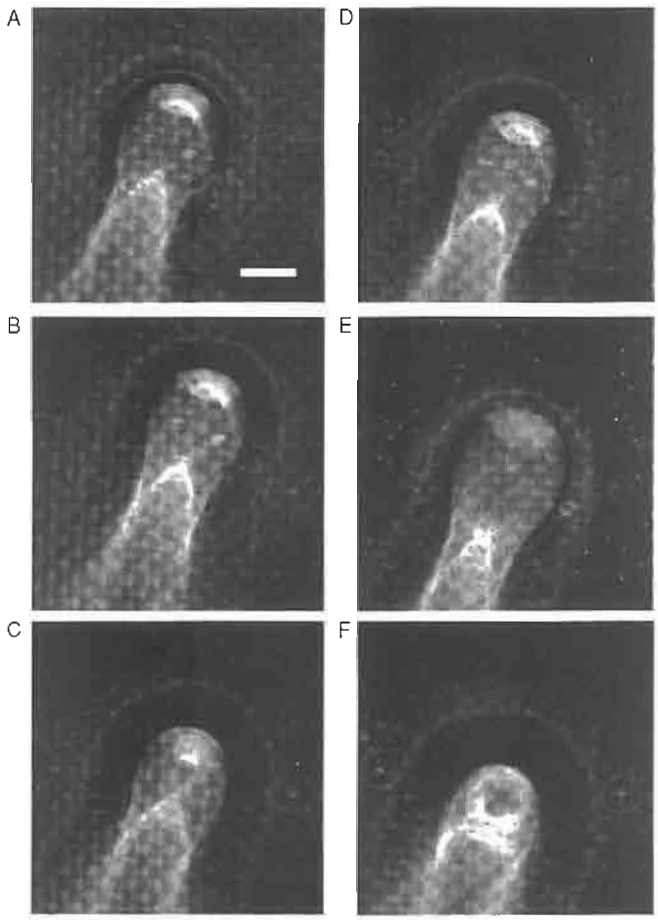

Fig. 6 Example images during the measurement of gel flexibility using spherically tipped microindentation. On initial indentation into a polyacrylamide gel, the image of the tip (B) is matched with the reference image (A), to make sure that the microscope is focusing on the bottom surface of the tip. The microindenter is then raised to a slightly higher position while remaining in contact with the sample (C). The new position of the tip and the gel surface are determined by serial optical sectioning and looking for an image that matches the reference image (D), and an image that shows sharply focused surface beads (E), respectively. The microscope focus is then returned to the point of initial indentation while the probe is raised off the sample surface (F). Serial optical sectioning is again performed to determine the position of the gel surface and the spherical tip off the surface. Scale bar is 25 μm.

1. Spinkle 1-μm fluorescent polystyrene beads (Molecular Probes) on the surface of the gel to be measured to mark the surface for focusing. A low density of beads is preferred ($\sim$2 beads/100 μm^2; Fig. 6E), as too high a density could interfere with the observation of the tip of the microindenter.

2. Set the microindenter to the angle it was calibrated. Rotate the microindenter such that the tip is pointing *down*. This is again confirmed by focusing the microscope up and down and by making sure that the lateral profile of the microindenter shows no kinks.

3. Estimate the thickness of the sample to make sure that it is at least 100 μm, which is required for reliable measurements of Young's modulus. This is done by using the calibrated focusing mechanism of the microscope, to focus from scratches or debris on the glass surface to the sprinkled fluorescent beads on the surface of the gel.

4. Use the micromanipulator to lower the microindenter until the tip starts to thrust forward, indicating that the tip is experiencing counter forces as it enters and exerts forces on the gel (Fig. 5). For optimal results (see below), the indentation, δ, should be $\sim 0.8r$, where r is the radius of the tip. The indentation may be estimated using the microscope focusing mechanism.

5. Focus the microscope until the phase-contrast image of the spherical tip (Fig. 6B) matches the reference image collected in Section IV.C (Fig. 6A). This focuses the microscope on the bottom surface of the spherical tip. This step may best be accomplished by taking serial image sections at <0.5-μm separation, searching for the best match within the image stack (note the two phase light dots near the tip), then moving the focal plane to the position where the best match with the reference image is found. The position is referred to as position A_1 (Fig. 5). Record a phase-contrast image of the spherical tip.

6. Raise the microindenter slightly, such that it is still indenting the sample but at a shallower depth, $>0.3r$ (Figs. 5 and 6C). This position is referred to as position A_2. Record the distance of vertical movement of the micromanipulator (z_1). Do not change the focus of the microscope.

7. Collect the first stack of optical sections, from position A_1 upward to somewhere above the surface of the gel (above the position in Fig. 6E), then return the microscope focus to the position A_1 using the focusing mechanism. If available, use a combination of transmitted and epi-illumination such that phase contrast and fluorescence are recorded as superimposed images.

8. Raise the tip of the microindenter such that it is above but not too far from the surface of the sample (Figs. 5 and 6F). This position is referred to as the off position or position A_3. Record the distance of vertical movement of the micromanipulator, z_2.

9. Collect a second stack of optical sections from position A_1 upward to somewhere above the spherical tip. If available, use a combination of transmitted and epi-illumination such that phase contrast and fluorescence are recorded as superimposed images.

10. In both stacks of optical sections, look for the section where the beads on the surface in the periphery of the image (i.e., away from the point of indentation) are in sharp focus (Fig. 6E). Calculate the corresponding position, which is referred to

as the surface position or positions B_1 and B_2, respectively (which theoretically should be at the same position, though B_2 is slightly more reliable due to the lack of indentation).

11. Search for the optical section in the first stack where the image of the tip matches the reference image (Fig. 6D). This marks the position of A_2. Distances B_1-A_1 and B_2-A_2 are the corresponding sample indentations, δ_1 and δ_2.

12. Search for the optical section in the second stack where the image of the tip matches the reference image. This marks the position of A_3, where the spherical tip is above the gel by a distance of H.

13. According to Fig. 5, the difference between $z_1 + z_2 - H$ and δ_1 is the net vertical deflection d_1 of the microindenter at position A_1, and the difference between $z_2 - H$ and δ_2 is the net vertical deflection d_2 of the microindenter at position A_2. However, direct measurement of H is prone to error due to surface interactions between the needle and the gel. A more reproducible approach is to plot the net deformation of the tip against the height of the micromanipulator $[z_1 + z_2, \sqrt{((A_3-A_1)^2 + y_1^2)}$, and $(z_2, \sqrt{(A_3-A_2)^2 + y_2^2)}]$, where y is any lateral deflection of the microindenter tip (Fig. 7). If $H = 0$, the line connecting these two points should pass through the origin while maintaining the same slope. Therefore, its x-intercept is used as the estimate of H. It is important that the final position of the tip A_3 be very close to, but not touching, the surface. This position should yield a nearly linear relationship between net tip deformation and applied force, a condition which is required for the analysis.

14. Using the value of k obtained from the calibration curve obtained in Section IV.C, convert d_1 and d_2 to forces f_1 and f_2. This generates two pairs of force–indentation relationships, f_1 and f_2, and the corresponding indentations δ_1 and δ_2.

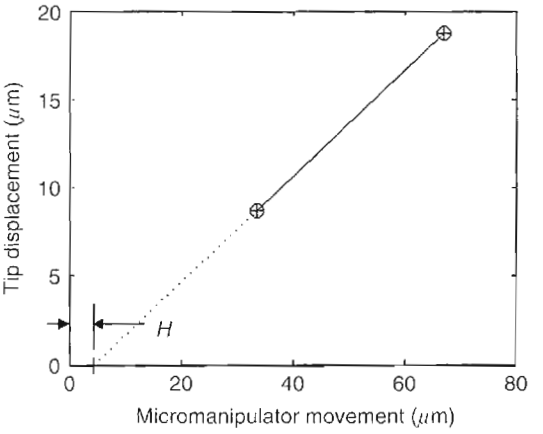

Fig. 7 Estimation of contact point from data taken on a polyacrylamide gel with 8% acrylamide and 0.08% bis.

15. Repeat the measurements at several different locations of the gel.

16. The microindenter may be stored and reused many times. Accumulated beads on the surface of the tip should be removed as much as possible by gentle sonication in a detergent solution, since they interfere with the phase-contrast imaging of the tip.

E. Data Analysis

Each set of f_1, δ_1 and f_2, δ_2 is first checked for consistency. The Young's modulus, E, is calculated for each pair of f, δ using the Hertz equation for a rigid sphere [Eq. (1); Fig. 8], assuming a Poisson's ratio of 0.45 for polyacrylamide (Engler *et al.*, 2004a). The resulting two Es should agree within 33% and those exceeding this criterion are removed. Inconsistency is typically due to one of the indentations being too deep or shallow (discussed later).

The use of the Hertz model is generally considered valid only for small indentations, due to behavior other than linear elasticity at greater indentation depths. However, macroscopic testing of polyacrylamide gels indicated that this limit may be overly conservative (Engler *et al.*, 2004a). AFM data with spherical tips also found good agreement to the Hertz model at indentations up to r (Engler *et al.*, 2004b). A similar conclusion was reached using conical tips, which involve higher strains that exceed this limit even at very low forces (Dimitriadis *et al.*, 2002; Engler *et al.*, 2004b). Most notably, Yoffe found that the Hertz model is valid to within 1%

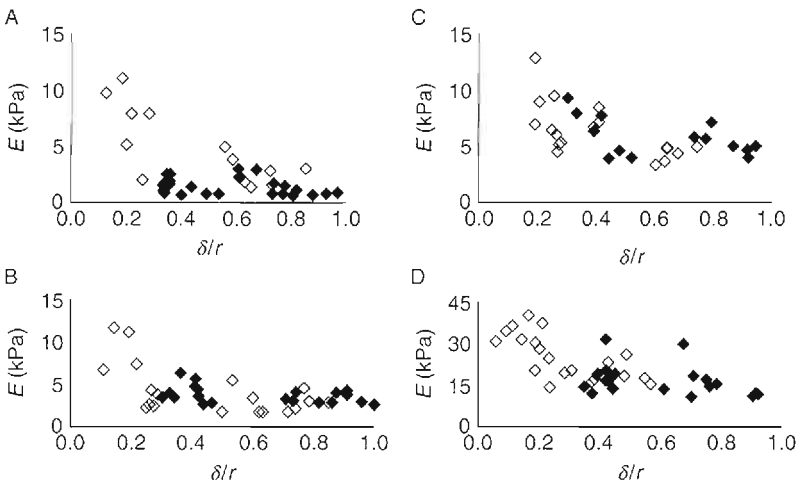

Fig. 8 Young's moduli of polyacrylamide samples calculated from discrete force-indentation data obtained with spherically tipped microindentation. The points that meet the selection criteria as described in the text are indicated by filled dots and those rejected by open dots. Data shows the upward trend of E at lower indentations for polyacrylamide gels made from 5% and 0.025% (A), 5% and 0.06% (B), 0.1% (C), and 8% and 0.08% (D) acrylamide and bis.

error for large indentations at least up to $a/r \sim 0.8$, where $a^2 = \delta r$ and a is the radius of the contact area, or $\delta \sim 0.64r$ for materials with a high Poisson's ratio (0.40; Yoffe, 1984). For the present measurements, Yoffe's correction for a material of $\nu = 0.40$ amounts to a difference of less than 2% in the value of E. These results suggest that indentations up to the radius of the microindenter may be applied in the present approach in conjunction with an uncorrected Hertz model, for elastic materials that are nearly incompressible (high ν).

At small indentations, significant systematic error does occur. For example, experimental measurements indicated larger measured contact areas than those predicted by the model at low indentations (Fessler and Ollerton, 1957; Johnson, 1985), which leads to a value of E that is several times higher than those measured at higher indentations. There may be additional sources of error at small δ, for example, from surface interactions between the probe and the sample. An upward trend in E at low δ is indeed observed in both the present measurement (Fig. 8), and in several studies with AFM (Dimitriadis *et al.*, 2002; Richert *et al.*, 2004), where the values at low indentation depths were found to be two to three times higher than those at higher indentation depths. This systematic error may also explain the higher values of E obtained with the bead indentation measurement as discussed in Section II, particularly for stiff gels where the indentation may be very small compared with the radius of the bead.

On the basis of above considerations, the calculation of E for spherical tip microindentation was performed for data with $\delta_1 < r$ and $\delta_2 > 0.3r$. Moreover, the sample should be thick enough to avoid potential stress-stiffening artifacts from the underlying glass substrate. The values of E derived from qualified data sets turned out to be relatively consistent (Fig. 8), and were averaged to obtain the final value. The results with several polyacrylamide gels of different stiffness, as controlled by the concentrations of acrylamide/bis-acrylamide, are shown in Fig. 9. These measurements were conducted using three different probes with tip radii between 29.7 and 40.0 μm, spring constants between 0.099 and 0.143 nN/nm, and gels $\sim$150 μm in thickness. The values are in excellent agreement with those obtained with AFM as reported in the literature and measured independently (Guo *et al.*, 2006).

F. Discussion

As with any method, there are several sources of uncertainty. Values for Poisson's ratio of polyacrylamide gels commonly seen in the literature range between 0.3 and 0.5, and thus are responsible for the largest relative uncertainty. We chose to use a value of 0.45, as this value yields the best fit between E values obtained with macroscopic and microscopic testing (Engler *et al.*, 2004a).

A second significant source of error is associated with vertical measurements of the microindenter position based on visual inspection of images. However, although the field depth for a dry lens is typically several micrometers, the vertical position of the microindenter may be determined to an accuracy better than 1.0 μm,

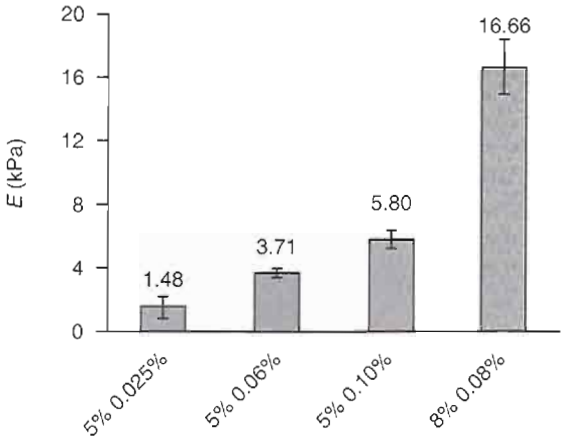

Fig. 9 Young's moduli for polyacrylamide gels of various stiffness obtained with spherically tipped microindentation, by averaging all the values that meet the selection criteria. Values are average ± SEM, $n = 10, 7, 10$, and 13.

using a stack of optical sections collected at ~0.25 μm per slice. The accuracy may be improved by replacing visual comparison with a cross-correlation-based algorithm for matching images. Other sources of error include the mechanical movements and calibration of the microscope-focusing mechanism and the micromanipulator (dial reading), the weight of the calibration wire, and the deviation of the tip from a perfect spherical shape. The relative uncertainties for the measurement of microindenter spring constant, deflection, gel indentation, and radius are estimated to be around 13%, 11%, 6%, and 1%, respectively. The net relative uncertainty for E is ~41% (18% contributed by method), which is within 5% of our estimate of the uncertainty for AFM measurements (Guo *et al.*, 2006).

Finally, the method is based on the assumption that the spherical tip glides freely (slips) on the gel surface as it applies forces, as obstruction in axial movements affects the bending behavior of the probe. Judging from the vertical and lateral distribution of beads on the surface, this obstruction appears to occur with very soft gels (<1 kPa), where the surface undergoes complex shape changes as the tip digs into the gel. A similar problem may affect AFM. Another assumption of this method is that all measurements are static since the time required for measurements is such that stress relaxation, if the material is viscoelastic, has likely already occurred.

There are many advantages to the spherically tipped microindenter method. It is straightforward and the analysis is simple. The materials and equipment are inexpensive compared to AFM, and are often available for other purposes. Once calibrated and if handled carefully, the microsphere indenter can be used repeatedly, in contrast to the much shorter longevity of expensive AFM probes because of cantilever damage or corrosion of the reflective coating. Although the build up of beads on the surface after repeated use can impair visualization of the tip

necessary for accurate measurements, the life of a microindenter can be extended greatly by cleaning after each use. This method also appears to be less sensitive to environmental factors than the AFM, as air currents and minimal amounts of vibration do not seem to significantly affect the outcome. This method can also test sticky samples that could not be tested with AFM due to its limited vertical scanner range necessary to pull the tip free from adhesive samples. One of the most significant advantages of this method is its ability to test substrates on a microscope, possibly in conjunction with the observations of cells. This is particularly useful for testing nonhomogenous substrates, and modulatable substrates that stiffen or soften in response to local manipulations. Even when used without quantification, it provides a convenient tool for assessing the mechanical properties of substrates during material development.

V. Conclusions

With the realization of the importance of mechanical signals, studies of cell biology are increasingly performed on polymer-based substrates with tunable mechanical properties in an effort to elucidate the mechanisms that regulate the complex cell behavior. The quality of these studies is directly affected by the proper characterization of the mechanical properties of these substrates.

While AFM represents a highly reliable and versatile approach, it is also the most costly and complicated compared to the two other methods. The optimization of AFM for high-resolution scanning of surfaces may in fact create unnecessary obstacles to the relatively simple task of stiffness measurements. This chapter shows that the measurements may be performed with much simpler and economical approaches. Indentation with microspheres is the easiest and cheapest method. Slightly more complicated but more reliable and versatile is the method of spherically tipped microindentation, which may be further improved by incorporating precise (e.g., piezoelectric) and automated positioning of the tip. Optimal choice of the method should take into consideration the requirements of the application, the acceptable uncertainty, as well as practical factors such as cost and equipment availability.

References

Bennig, G., Quate, C. F., and Gerber, C. (1986). Atomic force microscope. *Phys. Rev. Lett.* **56,** 930–933.

Dimitriadis, E. K., Horkay, F., Maresca, J., Kachar, B., and Chadwick, R. S. (2002). Determination of elastic moduli of thin layers of soft material using the atomic force microscope. *Biophys. J.* **82,** 2798–2810.

Domke, J., and Radmacher, M. (1998). Measuring the elastic properties of thin polymer films with the atomic force microscope. *Langmuir* **14,** 3320–3325.

Engler, A., Bacakova, L., Newman, C., Hategan, A., Griffin, M., and Discher, D. (2004a). Substrate compliance versus ligand density in cell on gel responses. *Biophys. J.* **86,** 617–628.

Engler, A., Richert, L., Wong, J. Y., Picart, C., and Discher, D. (2004b). Surface probe measurements of the elasticity of sectioned tissue, thin gels and polyelectrolyte multilayer films: Correlation between substrate stiffness and cell adhesion. *Surf. Sci.* **570,** 142–154.

Fessler, H., and Ollerton, E. (1957). Contact stresses in toroids under radial loads. *Br. J. Appl. Phys.* **8,** 387–393.

Guo, W. H., Frey, M. T., Burnham, N. A., and Wang, Y. L. (2006). Substrate rigidity regulates the formation and maintenance of tissues. *Biophys. J.* **90,** 2213–2220.

Hertz, H. J. (1882). Über die Berührung fester elastischer Körper. *J. Reine Angew. Mathematik* **92,** 156–171.

Jacot, J. G., Dianis, S., Schnall, J., and Wong, J. Y. (2006). A simple microindentation technique for mapping the microscale compliance of soft hydrated materials and tissues. *J. Biomed. Mater. Res. A* **79,** 485–494.

Johnson, K. L. (1985). "Contact Mechanics." Cambridge University Press, Cambridge.

Lee, J., Leonard, M., Oliver, T., Ishihara, A., and Jacobson, K. (1994). Traction forces generated by locomoting keratocytes. *J. Cell Biol.* **127,** 1957–1964.

Li, Y., Hu, Z., and Li, C. (1993). New method for measuring Poisson's ratio in polymer gels. *J. Appl. Polymer Sci.* **50,** 1107–1111.

Lo, C. M., Wang, H. B., Dembo, M., and Wang, Y. L. (2000). Cell movement is guided by the rigidity of the substrate. *Biophys. J.* **79,** 144–152.

Mahaffy, R. E., Shih, C. K., MacKintosh, F. C., and Kas, J. (2000). Scanning probe-based frequency-dependent microrheology of polymer gels and biological cells. *Phys. Rev. Lett.* **85,** 880–883.

Richert, L., Engler, A. J., Discher, D. E., and Picart, C. (2004). Elasticity of native and cross-linked polyelectrolyte multilayer films. *Biomacromolecules* **5,** 1908–1916.

Rotsch, C., Jacobson, K., and Radmacher, M. (1999). Dimensional and mechanical dynamics of active and stable edges in motile fibroblasts investigated by using atomic force microscopy. *Proc. Natl. Acad. Sci. USA* **96,** 921–926.

Sneddon, I. N. (1965). The relation between load and penetration in the axisymmetric Boussinesq problem for a punch of arbitrary profile. *Int. J. Eng. Sci.* **3,** 47–57.

Weisenhorn, A. L., Hansma, P. K., Albrecht, T. R., and Quate, C. F. (1989). Forces in atomic force microscopy in air and water. *Appl. Phys. Lett.* **54,** 2651–2653.

Yoffe, E. H. (1984). Modified Hertz theory for spherical indentation. *Philos. Mag. A* **50,** 813–828.

Zhao, Y. P., Shi, X., and Li, W. J. (2003). Effect of work of adhesion on nanoindentation. *Rev. Adv. Mater. Sci.* **5,** 348–353.